https://doi.org/10.5194/egusphere-2026-1415
Preprint. Discussion started: 8 April 2026

Is the volume-frequency distribution of eruptions a power-law? Accounting for volume uncertainty in modeling the size distribution of volcanic eruptions

Salvatore Ferrara[1], Jacopo Selva[2], Jacopo Natale[3], Warner Marzocchi[1,2]

[1]Modeling and Engineering Risk and Complexity, Scuola Superiore Meridionale, Naples, 80138, Italy
[2]Department of Earth, Environmental, and Resources Sciences, University of Naples Federico II, Naples, 80126, Italy
[3]Department of Earth and Geo-environmental Sciences, University of Bari Aldo Moro, Bari, 70125, Italy

Correspondence to: Salvatore Ferrara (salvatore.ferrara-ssm@unina.it)

Abstract. Forecasting the size of a future volcanic eruption in densely populated areas is a key aspect of volcanic hazard and risk assessment. Estimates of the next eruption's size for both long- and short-term forecasts are typically based on the sizes of past events. Using the erupted volume as a proxy for eruptive size, forecasts are often obtained from the sampling of a power-law distribution. Notwithstanding, the distribution of the measured/inferred erupted volume of past eruptions often appears markedly different from a power-law. Here, we consider how the uncertainty on the volume of past eruptions may affect the shape of a hypothetical power-law distribution. The goal is to understand if the distribution of real data is compatible with an Exponentially Modified Gaussian distribution (EMG) that includes both the power-law and the uncertainty on the observed volumes. We apply this method to two large high-risk calderas, Campi Flegrei, Italy, and Taupo, New Zealand, but it can be potentially applied to any volcano. We find that the EMG distribution provides a good statistical fit to both volcanoes' eruptive records, supporting the use of a power-law distribution for forecasting the volume of the next eruption.

1 Introduction

Quantifying volcanic hazard is not limited to just forecasting the time of the eruption onset. It must also take into account the size of events, as larger eruptions can create more hazardous phenomena that involve larger areas. The size of an eruption is therefore a parameter of fundamental importance for hazard and risk assessment. The use of an improper size distribution for future eruptions can lead to the underestimation or overestimation of the real hazard and risk, with serious implications both for the management of the volcanic crisis and for civilians' confidence in institutions and research bodies (Donovan and Oppenheimer, 2014). In volcanic systems, such as calderas, the size of eruptive events can vary by several orders of magnitude, and their distribution is one of the fundamental ingredients of both short- and long-term hazard quantification (Wright et al., 2019).

The central scientific question addressed in this paper is which size distribution should be used for volcanic hazard assessments. Here, we consider the erupted volume as a proxy for eruptive size. Assuming a constant density, the erupted volumes bring the same information as the total erupted mass (*TEM*). Owing to its wide variability, the *TEM* has been studied by its logarithm, as introduced by Pyle (2015):

https://doi.org/10.5194/egusphere-2026-1415
Preprint. Discussion started: 8 April 2026

$$M = \mathrm{Log}(TEM) - 7\ , \tag{1}$$

where M is the magnitude, and the TEM is expressed in kilograms. Using a logarithmic scale allows us to consider eruptive events that span in volume by several orders of magnitude, from small events to caldera-forming eruptions. We prefer the use of magnitude rather than the Volcanic Explosivity Index (VEI) defined by Newhall and Self (1982), as the latter has some limitations for including properly effusive eruptions and persistent or long-lasting activities (Pyle, 2015). In addition, it complicates the probabilistic model as the VEI scale is discrete, which makes its use not optimal for statistical inference purposes. On the other hand, the magnitude is a continuous scale that depends exclusively on the amount of erupted material; these characteristics make it more appropriate to model the size distribution of eruptions.

Many natural hazards, such as earthquakes, floods, and landslides, are dominated by frequent small events and progressively fewer large ones; for earthquakes, this behavior is captured by the Gutenberg–Richter law (Gutenberg and Richter, 1944), which predicts an exponential decline in frequency with increasing magnitude. Usually, the exponential behavior holds for a wide range of magnitudes, but it may have upper and lower roll-off due to physical constraints (Kagan, 1993; Malamud et al., 2004). By analogy, eruptive volumes are often modeled with a power-law distribution (Sandri et al., 2016; Papale et al., 2021), implying that small eruptions are far more likely than large ones (Simkin and Siebert, 1994). Yet it is easy to show that even simple plots of observed eruption volumes sometimes appear to deviate significantly from a power-law.

To investigate this discrepancy, we develop a probabilistic framework for the erupted volume distribution at Campi Flegrei and Taupo that explicitly accounts for measurement error in erupted volumes superimposed on a power-law model. Indeed, the uncertainty on past volumes/mass may be very large (Sulpizio et al., 2024) and may significantly impact the observed shape of the distribution. We then test whether this error-informed power-law adequately describes the observations satisfactorily; if so, the power-law remains the appropriate choice for hazard assessments as the apparent departures from past data can be explained by measurement uncertainty. Although the method is applied to a few specific volcanoes, we underline that the procedure is general enough to be applied to any volcano.

2. The theoretical power-law distribution

Since the magnitude of eruptions is defined as the logarithm of the mass (Eq. 1) (Pyle, 2015), a power-law on volumes or mass translates, by change of variable, into an exponential distribution on magnitude (Kagan, 1993). This relationship is analogous to the Gutenberg-Richter law for earthquakes, according to which the frequency of earthquakes decreases exponentially with increasing magnitude, as a consequence of the power-law distribution of the seismic moment. This exponential distribution is shifted, i.e., the magnitudes have a lower bound at M_{min}. This minimum magnitude refers to one minimum value that may be selected depending on the goal of the analysis. The most common definitions of the minimum magnitude are: the smallest eruption magnitude produced by the volcano, the minimum magnitude of interest, or the catalog's completeness magnitude, i.e., the threshold above which the catalog is considered complete. With this specification, the probability density function reads:

https://doi.org/10.5194/egusphere-2026-1415
Preprint. Discussion started: 8 April 2026

$$f_M = \begin{cases} \beta e^{-\beta(M-M_{min})} & M \geq M_{min} \\ 0 & M < M_{min} \end{cases}, \quad (2)$$

where $\beta = \frac{1}{\bar{M}-M_{min}}$ with $\bar{M}$ as the average magnitude (Aki, 1965). In line with our initial assumption, we can rewrite Eq. (2) in terms of a power-law on volumes or masses, following that $f_V = f_M \left|\frac{dM}{dV}\right|$. Eventually, we get:

$$f_V = \begin{cases} b V_{min}^b V^{-(b+1)} & V \geq V_{min} \\ 0 & V < V_{min} \end{cases}, \quad (3)$$

where $b = \frac{\beta}{\ln 10}$ and V_{min} is the minimum volume considered.

We test the appropriateness of the magnitude exponential distribution through the Lilliefors test (Lilliefors, 1967, 1969) and the Anderson-Darling test (AD test) (Anderson and Darling, 1952, 1954) (see Appendix). In both tests, the null hypothesis is that the real data are a random sample from the exponential distribution of Eq. (2) with the parameter β estimated from the data; the significance level chosen a priori for all tests performed is 0.01.

With a limited sample, rejection of the null hypothesis may chiefly reflect: (i) severe catalog incompleteness; (ii) substantial measurement error in volumes; or (iii) a true volume distribution that is not power-law/exponential. Hence, to investigate a physics-based explanation for a possible departure from a power-law behavior (hypothesis (iii)) of the measured volumes, we ought to check if one or both of the first hypotheses ((i) and (ii)) can explain such a departure.

Assessing the completeness of a single-volcano catalog is challenging due to limited data and the likely omission of small eruptions that are obscured by larger and/or younger events, which is also a function of their eruptive style. Adopting the exponential formulation of Eq. (2), the completeness magnitude must be smaller than the minimum considered magnitude M_{min}. Here, we first check the incompleteness through the existence of tephra deposits that cannot be attributed to any eruption with a defined volume, and we rely on the experts' judgment of volcanologists who built the catalog. Of course, small eruption deposits can be obliterated by larger eruptions, but this problem is mitigated if the minimum magnitude of interest is large enough. Indeed, the minimum magnitude for hazard purposes may be rather large, and if it is equal to (or larger than) the completeness magnitude, the problem of missing small eruptions becomes negligible.

Alternatively, the deviation from the exponential magnitude distribution may be the consequence of the error in the volume measurements. Volcanic deposits are, in fact, subject to erosion (Arnalds et al., 2013; Di Traglia et al., 2013) and burial, not to mention the uncertainty in the vent location and that the volume of the volcanic edifice prior to its erosion is often not considered in the calculation of the volumes of monogenic eruptions (Natale et al., 2026). These biases can introduce strong uncertainties in the volume estimation, which can have a typical error of about 70% for well-studied cases (Bonadonna et al., 2015) and up to a factor of 5 for the poorly characterized cases (Bonadonna and Costa, 2012; 2013), consequently impacting the magnitude estimation (Sulpizio et al., 2024). This may induce a large number of events to be artificially moved below the threshold defined by M_{min}, generating significant deviations from the power-law. By developing a statistical framework that accounts for volume uncertainty, we can get new clues on which one of these two hypotheses is more reliable.

https://doi.org/10.5194/egusphere-2026-1415
Preprint. Discussion started: 8 April 2026

3. Accounting for volume error

To account for the measurement uncertainty, we follow the procedure defined in Marzocchi et al. (2020); specifically, this procedure assumes that the observed magnitude (M^*) is the result of the true magnitude plus a normally distributed error: $M^* = M + \epsilon$ where $\epsilon \sim N(0, \sigma_M)$. As a consequence, we hypothesize that the data follow an exponentially modified Gaussian distribution (EMG), which is given by the convolution of a shifted exponential distribution and a normal distribution. The resulting pdf is given by:

$$f_{M^*} = \int_{M_{min}}^{\infty} \beta e^{-\beta(M - M_{\min})} \frac{1}{\sigma_M \sqrt{2\pi}} e^{-\frac{(M^* - M)^2}{2\sigma_M^2}} dM, \quad (4)$$

$$f_{M^*} = \frac{\beta}{2} e^{\frac{\beta}{2}(\beta\sigma_M^2 - 2(M^* - M_{min}))} \operatorname{erfc}\left[\frac{\beta\sigma_M^2 - (M^* - M_{min})}{\sigma_M \sqrt{2}}\right], \quad (5)$$

Since magnitude is a logarithmic function of volume, the volume error does not propagate linearly in the magnitude domain. If the volume is affected by a constant relative error $\epsilon_r = \frac{\sigma_V}{V}$ and ρ is the density of the magma, then the standard deviation of the magnitude is given by:

$$\sigma_M = \left|\frac{dM}{dTEM}\right| \sigma_{TEM} = \frac{1}{V\rho \ln(10)} \sigma_V \rho = \frac{\epsilon_r}{\ln(10)}, \quad (6)$$

By assuming a constant ϵ_r, thus a constant σ_M, the EMG distribution remains dependent on two parameters, β and M_{min}. In general, ϵ_r or equivalently σ_M should always be specified by the catalog producer to avoid overfitting. Estimating β and M_{min} through maximum likelihood estimation (MLE), we can fit the EMG distribution to the observed magnitudes. The estimation of both parameters does not consider the possible effects of incompleteness on this statistical distribution, which remains to be explored. This implies that M_{min} is the catalog-specific minimum magnitude above which the distribution appears exponential, rather than the theoretical lower bound at which it is exponential. If EMG fits well with the data, we can use the exponential distribution for forecasting, extending M_{min} to any value of interest.

4. Size distribution at Campi Flegrei

The Campi Flegrei caldera is a restless volcano and represents one of the highest-risk volcanic systems in the world, if not the highest, due to its complexity, its eruptive history (Orsi et al., 1996; Sparice et al., 2024), and its population density, overlapping with the metropolitan area of Naples. This volcanic field, throughout its history, has produced a very wide range of eruption sizes, from small monogenic events such as Monte Nuovo (Di Vito et al., 1987) to large magnitude eruptions, such as the Maddaloni/X-6 eruption at 109 ka (Fernandez et al., 2025), and the caldera-forming eruptions such as the Campanian Ignimbrite (CI) at 39 ka (Barberi et al., 1978; Giaccio et al., 2017) and the Neapolitan Yellow Tuff (NYT) at 15 ka (Orsi et al., 1992; Scarpati et al., 1993), which are the last of a series of very large eruptions in Middle-Late Pleistocene (Fernandez et al. 2024).

https://doi.org/10.5194/egusphere-2026-1415
Preprint. Discussion started: 8 April 2026

Eruption (CF)	Age (ka)	Volume DRE (km^3)	TEM (kg)	Magnitude
Monte Nuovo	0.49	0.03	7.2e+10	3.9
[1]Capo Miseno	3.8	0.15	3.6e+11	4.6
Fossa Lupara	3.8	0.07	1.7e+11	4.2
[1]Nisida	3.9	0.17	3.6e+11	4.6
Astroni 7	4.1	0.07	1.7e+11	4.2
Astroni 6	4.11	0.12	2.9e+11	4.5
Astroni 5	4.12	0.1	2.4e+11	4.4
Astroni 4	4.12	0.14	3.4e+11	4.5
Astroni 3	4.13	0.16	3.8e+11	4.6
Astroni 2	4.14	0.02	4.8e+10	3.7
Astroni 1	4.15	0.06	1.4e+11	4.2
Averno 2	4.28	0.07	1.7e+11	4.2
Solfatara	4.28	0.03	7.2e+10	3.9
Olibano	4.3	0.01	2.4e+10	3.4
Accademia	4.3	0.01	3.4e+10	3.5
Paleoastroni 3	4.4	0.02	4.8e+10	3.7
Santa Maria delle Grazie	4.44	0.01	2.4e+10	3.4
[4]Agnano-Monte Spina	4.55	3.2	7.6e+12	5.9
Paleoastroni 2	4.73	0.2	4.8e+11	4.7
Paleoastroni 1	4.79	0.05	1.2e+11	4.1
Monte Sant'Angelo	4.92	0.2	4.8e+11	4.7
Pignatiello 2	5.12	0.02	4.8e+10	3.7
Agnano 3	5.2	0.2	4.8e+11	4.7
Cigliano	5.25	0.05	1.2e+11	4.1
Averno 1	5.25	0.1	2.4e+11	4.4
Agnano 2	5.4	0.01	2.4e+10	3.4
Agnano 1	5.44	0.02	4.8e+10	3.7
San Martino	9.1	0.05	1.2e+11	4.1
Sartania 2	9.22	0.05	1.2e+11	4.1
Pigna San Nicola	9.35	0.3	7.2e+11	4.9
[3]Costa San Domenico	9.35	0.3	7.2e+11	4.9

https://doi.org/10.5194/egusphere-2026-1415
Preprint. Discussion started: 8 April 2026

Sartania 1	9.55	0.05	1.2e+11	4.1
Baia – Fondi di Baia	9.6	0.03	7.2e+10	3.9
[2,3]Porto Miseno	10.6	0.09	2.2e+11	4.3
[2,3]Bacoli	10.62	0.1	2.4e+11	4.4
Pisani 3	10.65	0.1	2.4e+11	4.4
Pignatiello 1	10.67	0.1	2.4e+11	4.4
Montagna Spaccata	10.7	0.02	4.8e+10	3.7
Concola	10.75	0.01	2.4e+10	3.4
Fondo Riccio	10.85	0.01	2.4e+10	3.4
Pisani 2	10.95	0.3	7.2e+11	4.9
Pisani 1	11.05	0.3	7.2e+11	4.9
Soccavo 5	11.15	0.1	2.4e+11	4.4
Minopoli 2	11.25	0.1	2.4e+11	4.4
Paleo San Martino	11.35	0.1	2.4e+11	4.4
Soccavo 4	11.45	0.3	7.2e+11	4.9
Soccavo 3	11.55	0.1	2.4e+11	4.4
Soccavo 2	11.65	0.1	2.4e+11	4.4
Paleo Pisani 2	11.65	0.3	7.2e+11	4.9
Paleo Pisani 1	11.75	0.1	2.4e+11	4.4
[2]Banco di Nisida	11.85	0.15	3.6e+11	4.6
[5]Pomici Principali	12	1.8	4.3e+12	5.6
Soccavo 1	12.2	0.5	1.2e+12	5.1
Minopoli 1	12.4	0.1	2.4e+11	4.4
Archiaverno	12.65	0.5	1.2e+12	5.1
Torre Cappella	12.9	0.05	1.2e+11	4.1
[2]La Pietra	13.5	0.2	4.8e+11	4.7
[3]Santa Teresa	13.7	0.03	7.2e+10	3.9
[3]Gauro	14.1	0.8	1.9e+12	5.3
Mofete	14.3	0.08	1.9e+11	4.3
Bellavista	14.3	0.4	9.6e+11	5.0
Rione Terra	14.3	0.1	2.4e+11	4.4
[3]Monteruscello	14.3	0.3	7.2e+11	4.9

https://doi.org/10.5194/egusphere-2026-1415
Preprint. Discussion started: 8 April 2026

Table 1: Age, DRE volume, Mass and Magnitude of post-NYT eruptions of Campi Flegrei (modified after Smith et al., 2011). [1] volume estimation after Natale et al. (2026); [2] stratigraphic position after Natale et al. (2022); [3] volume estimation made in this work based on [1]; [4] volume after Mele et al. (2020); [5] volume recalculated using Bonadonna and Houghton (2005).

Most of the eruptions since the NYT have occurred close in time, allowing the recent activity to be divided into three eruptive epochs (Di Vito et al., 1999). Epoch 1 is the one immediately following the NYT eruption (~14.3-10.6 ka), with 35 events mainly located along the caldera margins (Natale et al., 2024). This epoch is characterized mainly by small-to-moderate phreatomagmatic eruptions (Smith et al., 2011) and punctuated by more energetic events, such as the Pomici Principali eruption. Epoch 2 (~9.6-9.1 ka) was relatively shorter than the others and is characterized by just 6 eruptions. Epoch 3 (~5.4-3.8 ka) is characterized by 26 events and includes Agnano-Monte Spina (de Vita et al., 1999; Arienzo et al., 2010), the largest eruption of the volcano's post NYT record. The last eruption of the volcano was Monte Nuovo, which occurred in 1538 AD after a long period of quiescence (Di Vito et al., 1987).

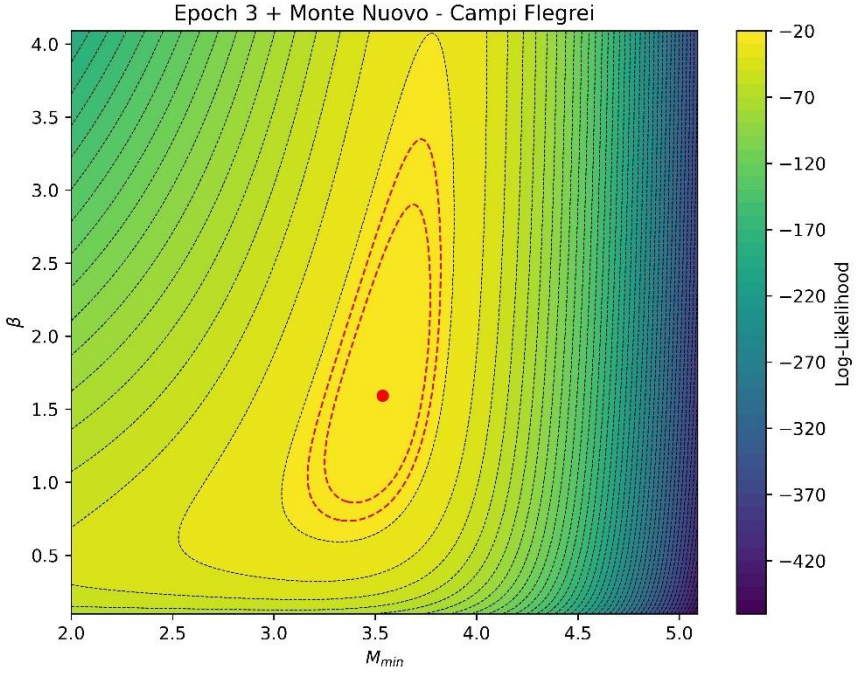

Figure 1: Log-Likelihood contour plot related to Campi Flegrei's eruptions (Epoch 3 + Monte Nuovo). The x-axis represents M_{min} while the y-axis represents β, the contour surfaces represent the Log-Likelihood values. The red dashed lines represent the 95th and 99th percentiles of the Log-Likelihood, while the red dot represents the couple of parameters that maximize it.

Despite the critical importance of the size of an eruption in assessing the hazard at Campi Flegrei, there is still a large gap in the scientific literature regarding its probabilistic forecast. Current models typically group the sizes of Campi Flegrei's eruptions into three classes (Orsi et al., 2009; Selva et al., 2018), but while this approach may be a good first-order

https://doi.org/10.5194/egusphere-2026-1415
Preprint. Discussion started: 8 April 2026

approximation, it neglects the intra-group variability, which may impact severely the volcanic hazard and risk assessment (Sandri et al., 2016).

To model the volume of the Campi Flegrei eruptions, we consider an updated post-NYT record (Table 1; eruption size and relative age updated from Smith et al., 2011; Pistolesi et al., 2017; Natale et al., 2022, 2026). We emphasize that five events in the original catalog from Smith et al. (2011) (La Pigna 1, La Pigna 2, Paradiso Tephra, Gaiola Tephra, Casale Tephra) currently do not have a defined volume, and are therefore not included in our dataset. The lack of these volumes represents a minimum estimate of the incompleteness of the catalog, as we cannot exclude that we may be missing additional data.

Applying the Lilliefors and AD tests, we reject the null hypothesis of exponentiality at the significance level chosen. This result is further supported by restricting the analysis to eruptions from the Epoch 3 eruptions plus Monte Nuovo activity (Selva et al., 2012): the Lilliefors test does not reject the null hypothesis at the chosen significance level, while the AD test rejects it. Overall, these results indicate that the exponential distribution is not a good descriptor of the magnitude distribution. We speculate that this discrepancy cannot be entirely attributed to catalog incompleteness.

Then, we test the hypothesis that the deviation from the expected trend is due to volume uncertainty using the EMG distribution. We first select the subset of the catalogue consisting of all Epoch 3 eruptions plus Monte Nuovo. This subset of 27 eruptions is often considered the most relevant for hazard assessment (Orsi et al., 2009). To calculate the magnitude, we consider a magma density of 2.4 gr cm^{-3} (Natale and Vitale, 2025). In this first application, we assume a relative error $\epsilon_r = 0.5$. Notably, $\epsilon_r = 0.5$ is lower than the relative errors reported for well-studied eruptions, which are typically around 70% (Bonadonna et al., 2015). This estimate also accounts for the uncertainty affecting volume calculations in complex systems such as calderas, including uncertainties in vent location, erosion, and submerged deposits. Applying the MLE (Fig. 1), we obtain:

- $M_{min} = 3.5 \pm 0.2$.
- $\beta = 1.6 \pm 0.8$.

We apply the AD and Lilliefors tests and obtain the *p*-value through a Monte Carlo simulation. Through Eqs. A.4 and A.5, we obtain *p*-values equal to 0.08 for the AD test and 0.28 for Lilliefors (both larger than the significance level chosen), so the EMG distribution cannot be rejected, that is, it is consistent with the observed data. Figure 2 shows (a) the probability density function and (b) the cumulative density function for the dataset of Epoch 3 plus Monte Nuovo. We perform the same tests using different relative errors to evaluate the sensitivity of the results. Assuming $\epsilon_r = 0.25$, we obtain *p*-values equal to 0.03 and 0.12, which are still higher than the chosen significance level. This means that the EMG distribution seems to be consistent with the data, even in the case of small errors. When $\epsilon_r = 0.75$ we get *p*-values equal to 0.22 and 0.93, both higher than the chosen significance level.

If we instead consider the entire post NYT record, we get:

- $M_{min} = 3.7 \pm 0.15$.
- $\beta = 1.5 \pm 0.5$.

https://doi.org/10.5194/egusphere-2026-1415
Preprint. Discussion started: 8 April 2026

Applying the AD and Lilliefors tests again, however, we reject the null hypothesis at the significance level chosen, so the EMG distribution is not consistent with the observed data if we consider the full catalog.

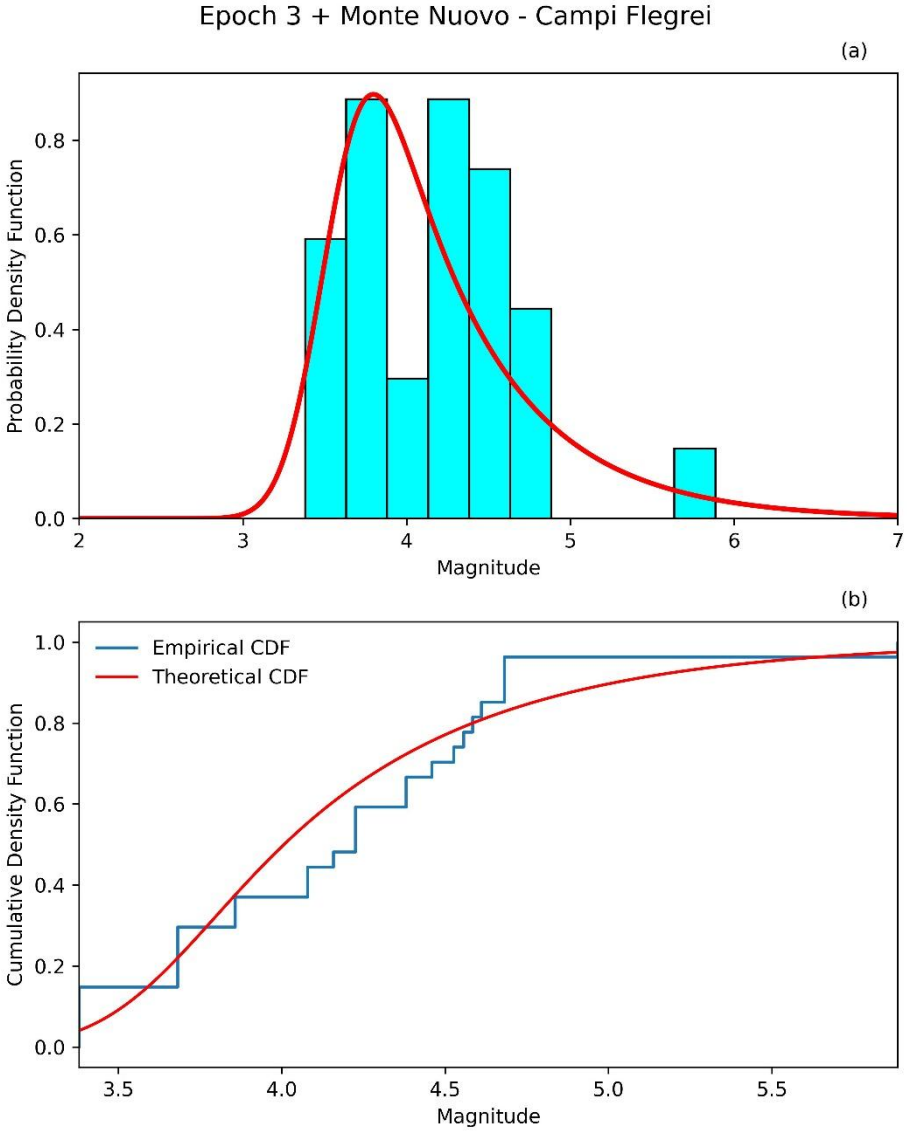

Figure 2: (a) Density histogram of Epoch 3 plus Monte Nuovo magnitudes of Campi Flegrei and EMG probability density function, for $\epsilon_r = 0.5$. (b) Empirical cumulative density function and theoretical EMG cumulative density function.

This means that the EMG does not seem to be consistent with observations only when the entire catalog is considered. We speculate that the most likely interpretation is a severe incompleteness or inhomogeneity of the catalog when its earliest part is included. To summarize, the results show that EMG is a suitable distribution for Campi Flegrei when the measurement error is realistic, and the most complete part of the catalog is considered.

https://doi.org/10.5194/egusphere-2026-1415
Preprint. Discussion started: 8 April 2026

5. Size distribution at Taupo

The Taupo caldera is located in the central part of the North Island of New Zealand and is part of the larger Taupo Volcanic Zone (TVZ). The most significant event in Taupo's eruptive history is the Oruanui eruption at 25.6 ka (Wilson et al., 2001, 2006), which produced several hundred km^3 of products, causing the caldera collapse that created the basin hosting Lake Taupo. After a period of quiescence following the Oruanui caldera-forming event, Taupo resumed its eruptive activity, producing a total of 28 eruptions (Wilson, 1993). Among the eruptions following Oraunui, the first three were dacitic and occurred between ~20.5-17 ka, while the other twenty-five, starting from ~12 ka, were rhyolitic (Barker et al., 2021) and occurred more closely together in time. The most recent explosive eruption at Taupo is Hatepe or "Taupo Eruption" (232 ± 10 AD), a very powerful eruption that produced large pyroclastic flows and further caldera collapse (Davy and Caldwell, 1998). The last eruption of the volcano, which has been labeled as “Z” (Wilson et al., 1993), occurred about 80 years after Hatepe.

Eruption (Taupo)	Age (ka)	Volume DRE (km^3)	TEM (kg)	Magnitude
Z	1.69	0.28	6.9e+11	4.8
Hatepe	1.77	35	8.6e+13	6.9
X	2.15	0.4	9.8e+11	5.0
W	2.75	0.023	5.6e+10	3.8
V	2.8	0.4	9.8e+11	5.0
U	2.85	0.1	2.4e+11	4.4
T	3.2	0.05	1.2e+11	4.1
S	3.55	7.5	1.8e+13	6.3
R	4.45	0.05	1.2e+11	4.1
Q	4.55	0.15	3.7e+11	4.6
P	4.75	0.05	1.2e+11	4.1
O	4.8	0.05	1.2e+11	4.1
N	4.85	0.15	3.7e+11	4.6
M	5.25	0.2	4.9e+11	4.7
L	5.3	0.07	1.7e+11	4.2
K	5.35	0.35	8.6e+11	4.9
J	5.37	0.015	3.7e+10	3.6
I	5.95	0.02	4.9e+10	3.7
H	6.05	0.08	2.0e+11	4.3
G	6.65	0.2	4.9e+11	4.7
F	7.05	0.07	1.7e+11	4.2

https://doi.org/10.5194/egusphere-2026-1415
Preprint. Discussion started: 8 April 2026

E	9.95	2.0	4.9e+12	5.7
D	11.38	0.1	2.4e+11	4.4
C	11.4	0.3	7.4e+11	4.9
B	11.8	0.5	1.2e+12	5.1
A	17	0.004	9.8e+09	3.0
Omega	18.8	0.05	1.2e+11	4.1
Psi	20.5	0.02	4.9e+10	3.7
Oruanui	25.58	530	1.3e+15	8.1

Table 2: Age, DRE volume, Mass and Magnitude of post-Oruanui eruptions of Taupo (from Barker et al., 2021, and references therein).

Its recent unrest episode (Potter et al., 2015; Illsley-Kemp et al., 2021; Lamb et al., 2024) and eruptive history make the Taupo caldera an extremely interesting object of study for volcanic hazard and risk assessment. Similar to what was previously seen for Campi Flegrei, there is a gap in the scientific literature regarding the probabilistic forecast of the size of the next Taupo eruption.

The Lilliefors and AD tests on the Taupo eruptions (Table 2) reject the null hypothesis of exponentiality at the significance level chosen. If we consider the last phase of activity of Taupo (~12 ka) (Barker et al., 2021), we reject the null hypothesis with Lilliefors, but not with AD. As we saw for Campi Flegrei, the exponential distribution does not represent a good fit for the Taupo magnitudes overall.

To model the magnitude of Taupo eruptions with EMG, we first consider the last 12 ka of activity and a constant density of 2.45 gr cm^{-3}. Analogously to Campi Flegrei, we assume $\epsilon_r = 0.5$, and through MLE (Fig. 3) we obtain:

- $M_{min} = 3.9 \pm 0.2$.
- $\beta = 1.3 \pm 0.6$.

We apply the AD and Lilliefors tests to the Taupo erupted volumes, and we obtain a *p*-value equal to 0.8 and 0.7; so, also in this case, the observed data are consistent with the EMG distribution. Figure 4 shows (a) the probability density function and (b) the cumulative density function for the dataset consisting of the last 12 ka of activity of the caldera. Assuming $\epsilon_r = 0.25$, the *p*-values decrease to 0.19 and 0.11, while when $\epsilon_r = 0.75$, we get *p*-values equal to 0.97 and 0.95. In all cases, the null hypothesis of the EMG distribution cannot be rejected.

If we consider the full catalog, we get:

- $M_{min} = 3.6 \pm 0.25$.
- $\beta = 1.0 \pm 0.4$.

https://doi.org/10.5194/egusphere-2026-1415
Preprint. Discussion started: 8 April 2026

We then apply the AD test and obtain *p*-values equal to 0.21 and 0.08, meaning that, also in this case, the EMG distribution is consistent with the data. If $\epsilon_r = 0.25$, the *p*-values decrease to 0.006 and 0.009, while for $\epsilon_r = 0.75$, we get *p*-values equal to 0.79 and to 0.43. The null hypothesis of EMG distribution is rejected only when $\epsilon_r = 0.25$.

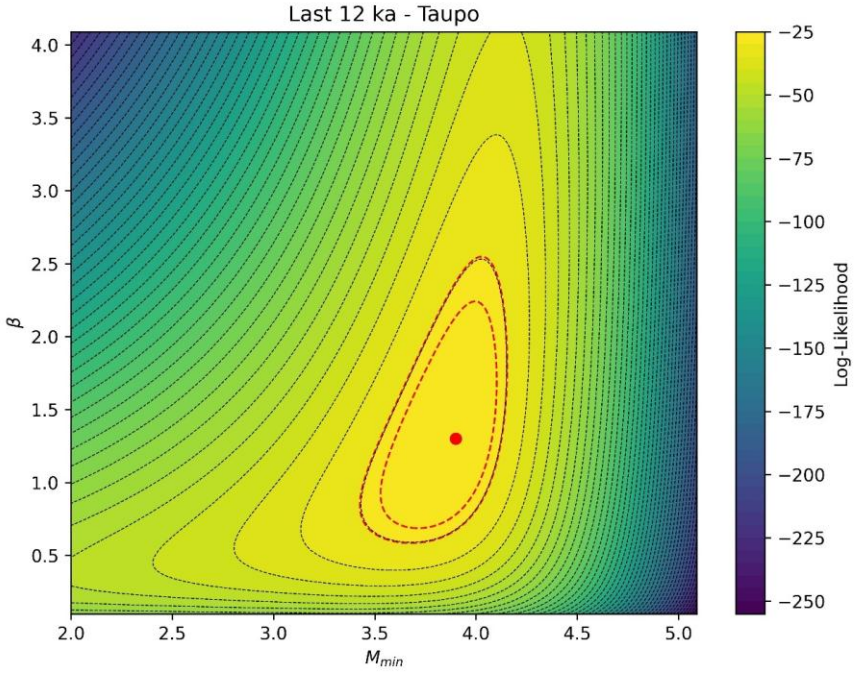

Figure 3: Log-Likelihood contour plot related to Taupo's eruptions (last 12 ka). The x-axis represents M_{min}, while the y-axis represents β, the contour surfaces represent the Log-Likelihood values. The red dashed lines represent the 95th and 99th percentiles of the Log-Likelihood, while the red dot represents the couple of parameters that maximize it.

In this case, a detailed assessment of catalog completeness is not feasible. However, the parameters for Taupo closely match those for Campi Flegrei, suggesting that any catalog incompleteness, if present, does not substantially bias the parameter estimates.

https://doi.org/10.5194/egusphere-2026-1415
Preprint. Discussion started: 8 April 2026

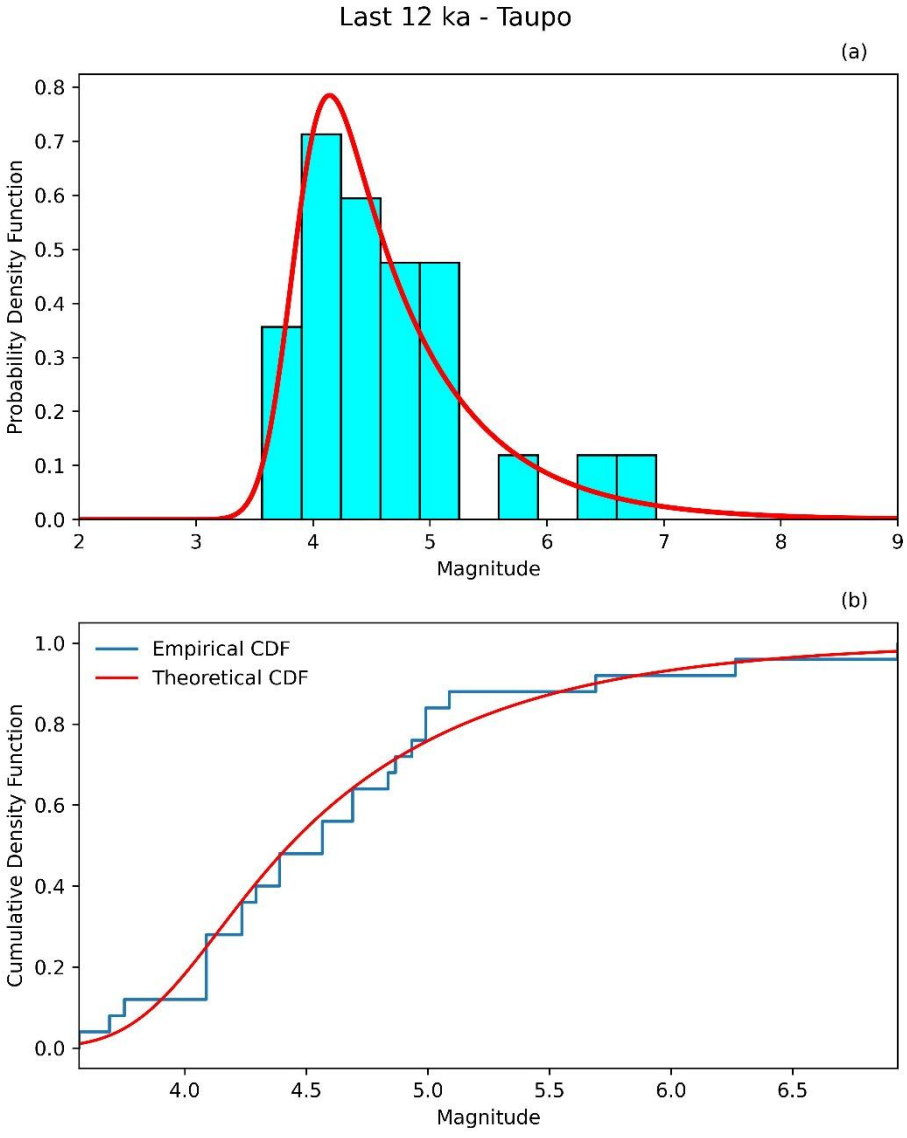

Figure 4: (a) Density histogram of the last 12 ka of activity of Taupo's eruption magnitudes and EMG probability density function, for $\epsilon_r = 0.5$. (b) Empirical cumulative density function and theoretical EMG cumulative density function.

6. Forecasting the size of future eruptions

When the catalog is not affected by clear incompleteness and the measurement error is realistic, the EMG distribution provides a statistically reliable fit to the magnitude of both the Campi Flegrei and Taupo eruptions for the time frame we have considered. Hence, the results of this work support that a power-law, or equivalently the exponential distribution of Eq. (2), can be used to forecast the volume or magnitude of the next eruption. The exponential distribution is characterized by the parameters β and M_{min}. In forecasting mode, β can be estimated via MLE, while M_{min} should be defined according to the

https://doi.org/10.5194/egusphere-2026-1415
Preprint. Discussion started: 8 April 2026

application's needs. When the catalog is incomplete, the estimated M_{min} may exceed the minimum magnitude of interest for hazard purposes, or the minimum magnitude capable of reactivating the volcanic system. In such cases, we can still use a shifted exponential model by adopting an application-driven M_{min} aligned with our goals. This requires assuming that the distribution is exponential, also for magnitudes smaller than the M_{min} estimated from past data, and that β is not significantly biased by incompleteness.

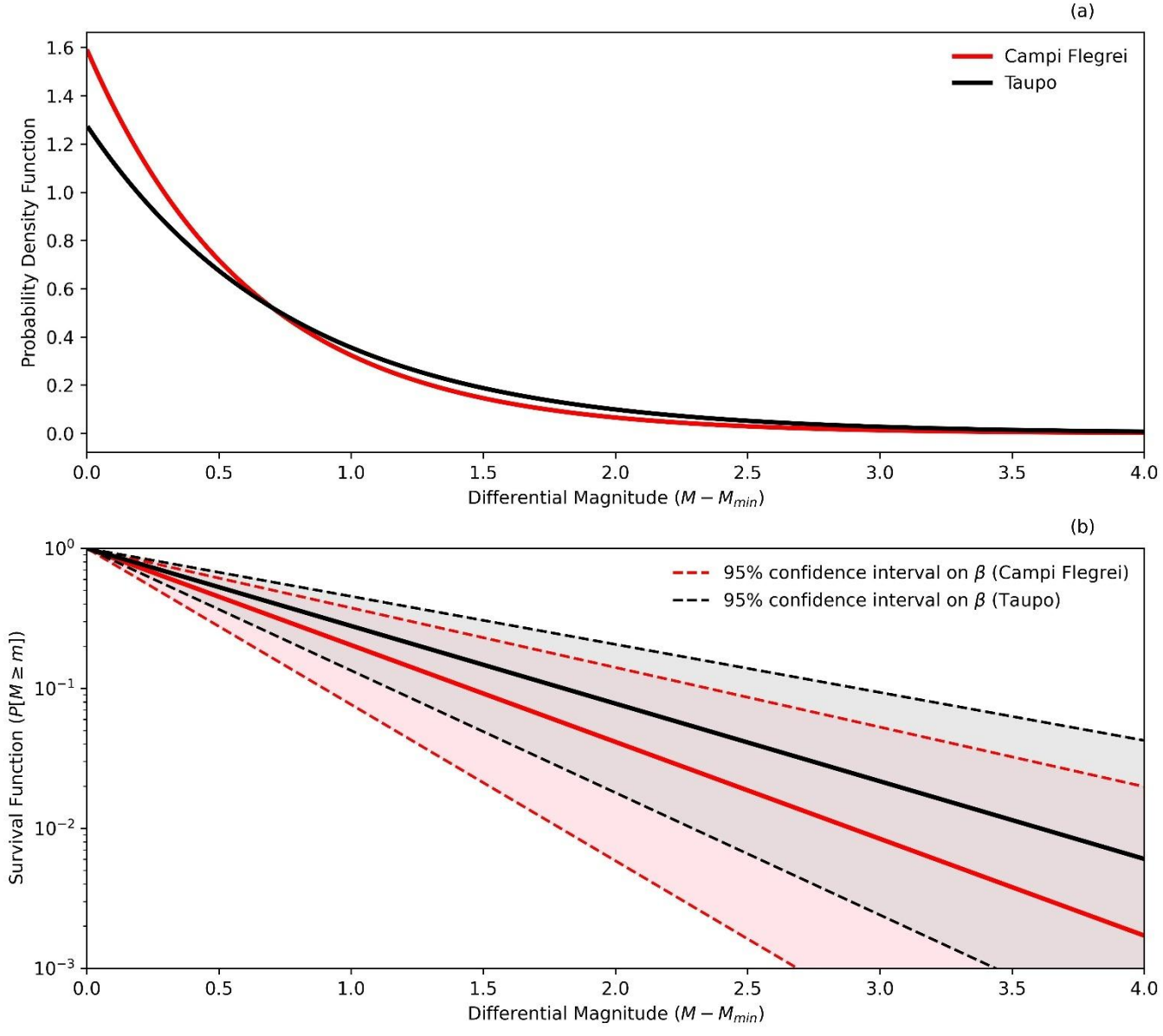

Figure 5: (a) Exponential probability density functions and (b) survival functions related to the magnitudes of Campi Flegrei and Taupo eruptions. The magnitudes reported on the x-axis have been shifted by the corresponding M_{min} to highlight the differences between the curves relating to the two volcanoes. The colored areas between the dashed lines represent a 95% confidence interval on β derived from the uncertainty related to the MLE.

https://doi.org/10.5194/egusphere-2026-1415
Preprint. Discussion started: 8 April 2026

Figure 5 shows (a) the exponential probability density functions and (b) the survival functions (exceedance probabilities, $P[M \geq m]$) derived from the estimated parameters for the datasets related to the most recent activity of both volcanoes, for a generic M_{min}. These distributions can be used to forecast the magnitude of the next eruption at each volcano, accounting for parameter uncertainty, we can estimate the epistemic uncertainty on this forecasting curve. Figure 5 illustrates that the mean exceedance probability for Campi Flegrei (red line) decreases more rapidly than that for Taupo (black line), which aligns with its higher mean β value. However, the epistemic uncertainty of the parameters indicates significant overlap in the survivor functions, suggesting the possibility of a common (or very similar) β for both volcanoes.

7. Conclusions and perspectives

In this work, we have developed a probabilistic framework to model the size of Campi Flegrei and Taupo's eruptions in terms of magnitude (Pyle, 2015). We have used the EMG distribution, which takes into consideration an exponential distribution and a normally distributed measurement error on magnitudes. Using realistic values of the uncertainty on the measure of volumes, the results show that the EMG distribution is statistically consistent with the observed magnitudes. Such a distribution is incompatible with the data only in cases of low error assumptions and/or incompleteness of the catalog. The compatibility of the data with EMG distribution implies that the null hypothesis of the magnitude exponential distribution cannot be rejected by the observations; i.e., small-magnitude eruptions are the most likely, and the probability of larger magnitude eruptions, up to the very large Neapolitan Yellow Tuff, Campanian Ignimbrite, Hatepe, or Oruanui, cannot be ruled out, even if they are unlikely events. This is consistent with the expectation that natural phenomena tend to occur more frequently at low intensities (Gutenberg and Richter, 1944; Simkin and Siebert, 1994). Furthermore, the use of a continuous distribution overcomes the limitations of using groups of discrete eruption sizes (Orsi et al., 2009; Selva et al., 2018), which ignore the variability inside each class, or other induced discontinuities introduced when intra-class variability is superimposed on a distribution based on classes (Sandri et al., 2016); de facto, this aspect may have a major impact on volcanic hazard estimations. Although we have applied this methodology to Campi Flegrei and Taupo, we underline that this method can be applied to any volcano of interest. The application of EMG to Campi Flegrei and Taupo shows that, in both cases, the apparently non-exponential distribution of past eruptions may be caused by uncertainty in the estimation of past volumes. The minimum magnitude for which exponentiality seems to hold overlaps for the two volcanoes. On the other hand, the estimated β values for these two calderas are considerably lower than the average β value of 3.5 derived from global catalogs (Papale et al., 2021). This may imply that the power-law parameter for these calderas differs from that obtained for volcanoes worldwide. Conversely, it may also be explained by undetected severe incompleteness in both catalogs.

Appendix

The Lilliefors test (Lilliefors, 1967, 1969) is a statistical test that tests the null hypothesis that a sample of data is drawn from a normal or exponential distribution. It is based on the Kolmogorov-Smirnov test (KS test) (Massey, 1951), from which it differs in that the null hypothesis does not specify the parameters of the distribution. Therefore, the Lilliefors test is more suitable than the KS test when the distribution parameters are estimated from the data. Lilliefors' test statistic is:

https://doi.org/10.5194/egusphere-2026-1415
Preprint. Discussion started: 8 April 2026

$$D = \sup_x \left|\hat{F}_x - F_x\right|, \tag{A.1}$$

where $\hat{F}_x$ is the empirical cumulative density function and F_x is the theoretical cumulative density function. The statistic is finally compared with the specific tabulated values for the Lilliefors test to obtain the *p*-value.

The Anderson-Darling test (AD test) (Anderson and Darling, 1952, 1954) also tests the hypothesis that a sample of data comes from a certain type of distribution. The statistic of the AD test is:

$$A^2 = -n - S, \tag{A.2}$$

where *n* is the sample size and:

$$S = \sum_{i=1}^{n} \frac{2i-1}{n} [ln(F_x) + ln(1 - F_{x_{n+1-i}})], \tag{A.3}$$

The test statistic is then compared to specific critical values for the distribution being tested. If it is greater than the corresponding critical value, then the null hypothesis must be rejected.

However, critical values for the AD and Lilliefors tests do not exist for the EMG distribution we adopted, but we can estimate the *p*-value via Monte Carlo simulation, generating *N* samples from the theoretical EMG model and comparing the observed statistics with those of the synthetic samples:

$$p = \frac{1}{N} \sum_{i=1}^{N} \mathbb{I}(D_i \geq D_{obs}), \tag{A.4}$$

$$p = \frac{1}{N} \sum_{i=1}^{N} \mathbb{I}(A_i^2 \geq A_{obs}^2), \tag{A.5}$$

where D_i and A_i^2 are the Lilliefors and AD statistics of the *i*-th sample, D_{obs} and A_{obs}^2 are the statistics of the observed data, and $\mathbb{I}$ is the indicator function, which is equal to 1 if $D_i \geq D_{obs}$ or $A_i^2 \geq A_{obs}^2$ and 0 otherwise.

https://doi.org/10.5194/egusphere-2026-1415
Preprint. Discussion started: 8 April 2026

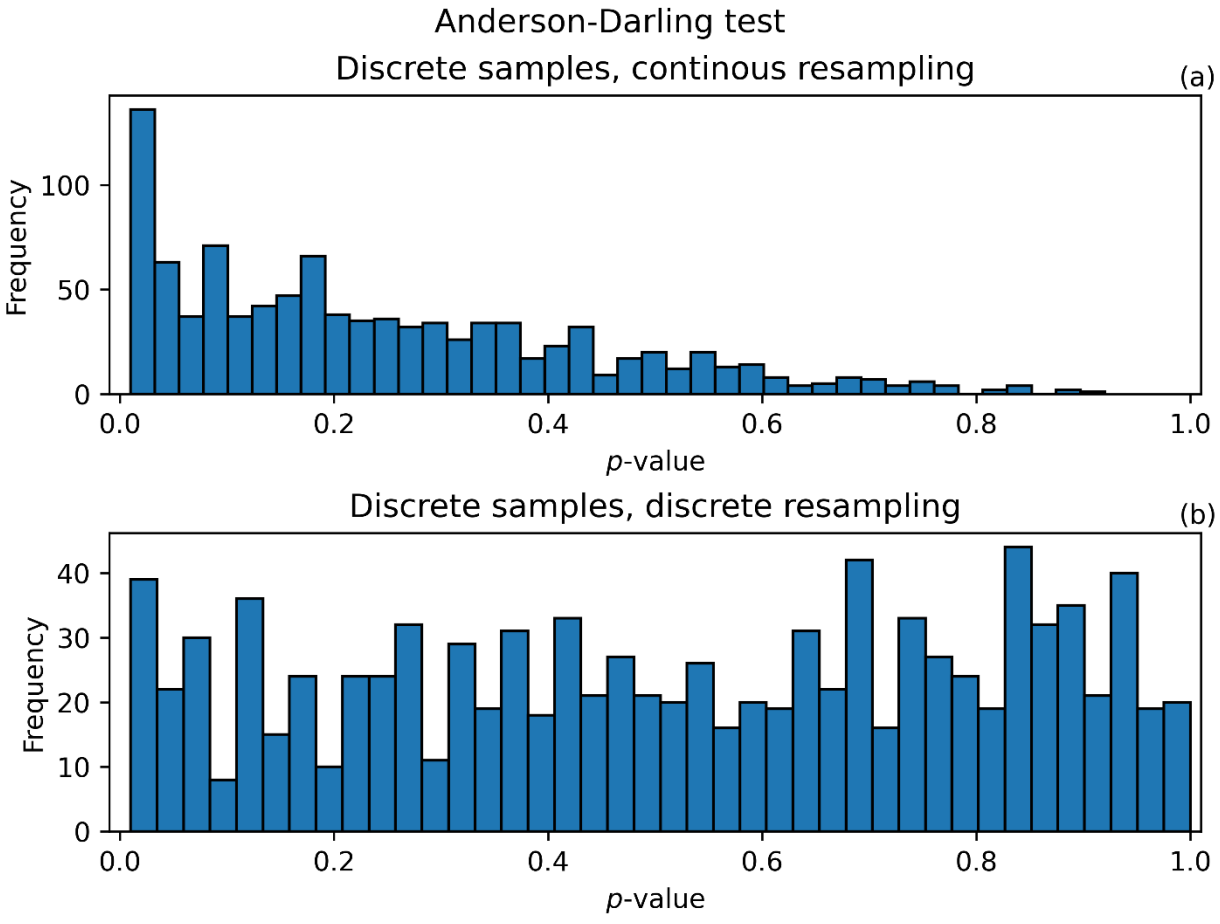

Figure A.1: Distribution of *p*-values (AD test) for discrete samples obtained by generating (a) continuous and (b) discretized samples via Monte Carlo simulation.

Although the size of volcanic eruptions is a continuous random variable, the catalogs we use are discretized due to the rounding of the volume measures (see Tables 1, 2). Consequently, generating continuous samples for *p*-value calculation via Monte Carlo simulation generates a non-uniform distribution under the null hypothesis, with a relative overabundance of low *p*-values that may result in the rejection of the hypothesis even in the absence of sufficient statistical evidence (Type 1 Error) (see Fig. A.1 (a), A.2 (a)). To account for this characteristic of the observed data, the Monte Carlo procedure for calculating the *p*-value is implemented by applying to the simulated samples the same discretization as the starting sample, rounding the magnitude values of the generated samples to the nearest values from the original data for magnitudes lower than 5. For magnitudes higher than 5, the simulated samples are left continuous, as the catalogs do not present such discretization above this value. Figures A.1 (b), A.2 (b) show how, by implementing this measure, the distribution of *p*-values under the null hypothesis is uniform.

https://doi.org/10.5194/egusphere-2026-1415
Preprint. Discussion started: 8 April 2026

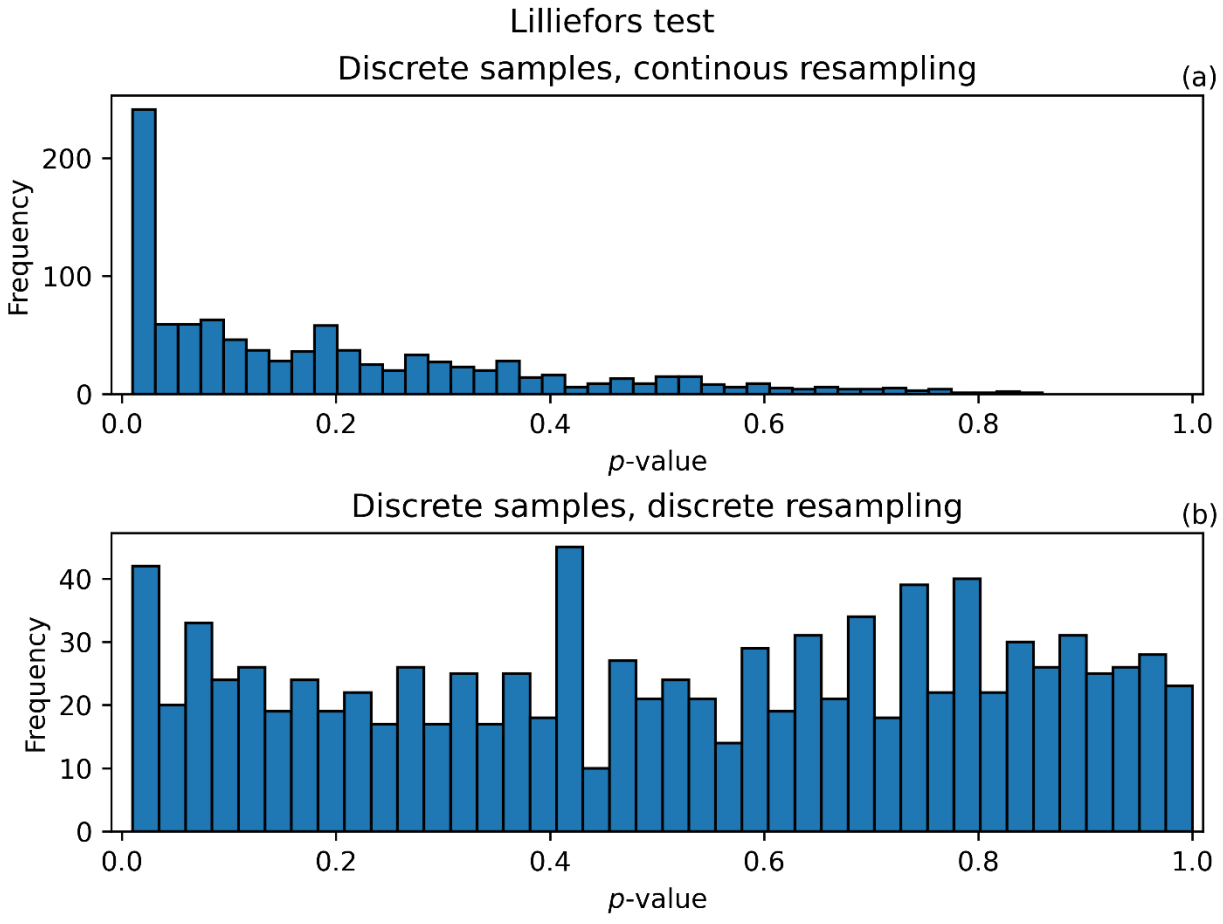

Figure A.2: Distribution of *p*-values (Lilliefors test) for discrete samples obtained by generating (a) continuous and (b) discretized samples via Monte Carlo simulation.

Code and data availability

Model code available upon request to the authors. The Campi Flegrei catalog has been modified after Smith et al. (2011) (https://doi.org/10.1016/j.quascirev.2011.07.012), while the Taupo catalog is reported in Barker et al. (2021) (https://doi.org/10.1080/00288306.2020.1792515).

Author contributions

SF, JS, and WM designed the model. JN recalculated the volumes of Campi Flegrei's eruptions and provided the full catalog. SF developed the model code and prepared the manuscript with the contribution of all authors.

https://doi.org/10.5194/egusphere-2026-1415
Preprint. Discussion started: 8 April 2026

Competing interests

Authors declare no competing interests.

Acknowledgements

All calculations were performed in Python using the following libraries: NumPy, pandas, SciPy, and statsmodels. The figures were also produced in Python with the Matplotlib library.

Financial support

This study was carried out within the Centro Pericolosità Vulcanica (CPV) project.

References

Aki, K.: A note on the use of microseisms in determining the shallow structure of the Earth's crust, *Geophysics*, 30, 665–666, https://doi.org/10.1190/1.1439640, 1965.

Anderson, T. W. and Darling, D. A.: Asymptotic theory of certain goodness-of-fit criteria based on stochastic processes, *Ann. Math. Stat.*, 23, 193–212, 1952.

Anderson, T. W. and Darling, D. A.: A test of goodness of fit, *J. Am. Stat. Assoc.*, 49, 765–769, 1954.

Arienzo, I., Moretti, R., Civetta, L., Orsi, G., and Papale, P.: The feeding system of the Agnano–Monte Spina eruption (Campi Flegrei, Italy): Dragging the past into present activity and future scenarios, *Chem. Geol.*, 270, 135–147, https://doi.org/10.1016/j.chemgeo.2009.11.012, 2009.

https://doi.org/10.5194/egusphere-2026-1415
Preprint. Discussion started: 8 April 2026

Arnalds, Ó., Þórarinsdóttir, E. F., Þórsson, J., Dagsson-Waldhauserová, P., and Ágústsdóttir, A. M.: An extreme wind erosion event of the fresh Eyjafjallajökull 2010 volcanic ash, *Sci. Rep.*, 3, 1257, https://doi.org/10.1038/srep01257, 2013.

Barberi, F., Innocenti, F., Lirer, L., Munno, R., Pescatore, T., and Santacroce, R.: The Campanian ignimbrite: a major prehistoric eruption in the Neapolitan area (Italy), *Bull. Volcanol.*, 41, 10–31, https://doi.org/10.1007/BF02597680, 1978.

Barker, S. J., Wilson, C., Illsley-Kemp, F., Leonard, G. S., Mestel, E., Mauriohooho, K., and Charlier, B. L. A.: Taupō: an overview of New Zealand's youngest supervolcano, *N. Z. J. Geol. Geophys.*, 64, 320–346, https://doi.org/10.1080/00288306.2020.1792515, 2021.

Bonadonna, C. and Costa, A.: Estimating the volume of tephra deposits: a new simple strategy, *Geology*, 40, 415–418, https://doi.org/10.1130/G32769.1, 2012.

Bonadonna, C. and Houghton, B. F. Total grain-size distribution and volume of tephra-fall deposits. Bulletin of Volcanology, 67(5), 441-456, https://doi.org/10.1007/s00445-004-0386-2, 2005.

Bonadonna, C. and Costa, A.: Plume height, volume, and classification of explosive volcanic eruptions based on the Weibull function, *Bull. Volcanol.*, 75, 742, https://doi.org/10.1007/s00445-013-0742-1, 2013.

Bonadonna, C., Biass, S., and Costa, A.: Physical characterization of explosive volcanic eruptions based on tephra deposits: propagation of uncertainties and sensitivity analysis, *J. Volcanol. Geotherm. Res.*, 296, 80–100, https://doi.org/10.1016/j.jvolgeores.2015.03.009, 2015.

Davy, B. and Caldwell, T. G.: Gravity, magnetic and seismic surveys of the caldera complex, Lake Taupo, North Island, New Zealand, *J. Volcanol. Geotherm. Res.*, 81, 69–89, https://doi.org/10.1016/S0377-0273(97)00074-7, 1998.

de Vita, S., Orsi, G., Civetta, L., Carandente, A., D'Antonio, M., Deino, A. L., di Cesare, T., Di Vito, M. A., Fisher, R. V., Isaia, R., Marotta, E., Necco, A., Ort, M. H., Pappalardo, L., Piochi, M., and Southon, J.: The Agnano–Monte Spina eruption (4100 years BP) in the restless Campi Flegrei caldera (Italy), *J. Volcanol. Geotherm. Res.*, 91, 269–301, https://doi.org/10.1016/S0377-0273(99)00039-6, 1999.

Di Vito, M. A., Lirer, L., Mastrolorenzo, G., and Rolandi, G.: The 1538 Monte Nuovo eruption (Campi Flegrei, Italy), *Bull. Volcanol.*, 49, 608–615, https://doi.org/10.1007/BF01079966, 1987.

Di Vito, M.A., Isaia, R., Orsi, G., Southon, J.D., De Vita, S., D'Antonio, M., Pappalardo, L., and Piochi, M.: Volcanism and deformation since 12,000 years at the Campi Flegrei caldera (Italy), Journal of Volcanology and Geothermal Research, v. 91, no. 2–4, p. 221–246, https://doi.org/10.1016/S0377-0273(99)00037-2, 1999.

Di Traglia, F., Pistolesi, M., Rosi, M., Bonadonna, C., Fusillo, R., and Roverato, M.: Growth and erosion: the volcanic geology and morphological evolution of La Fossa (Island of Vulcano, Southern Italy) in the last 1000 years, *Geomorphology*, 194, 94–107, https://doi.org/10.1016/j.geomorph.2013.04.018, 2013.

Donovan, A. and Oppenheimer, C.: Science, policy and place in volcanic disasters: insights from Montserrat, *Environ. Sci. Policy*, 39, 150–161, https://doi.org/10.1016/j.envsci.2013.08.009, 2014.

https://doi.org/10.5194/egusphere-2026-1415
Preprint. Discussion started: 8 April 2026

Fernandez, G., Giaccio, B., Costa, A., Monaco, L., Nomade, S., Albert, P. G., et al.: New constraints on the Middle–Late Pleistocene Campi Flegrei explosive activity and Mediterranean tephrostratigraphy, *Quat. Sci. Rev.*, 331, 108623, https://doi.org/10.1016/j.quascirev.2024.108623, 2024.

Fernandez, G., Costa, A., Giaccio, B., Natale, J., Palladino, D.M., and Sottili, G.: The Maddaloni/X-6 eruption stands out as one of the major events during the late Pleistocene at Campi Flegrei: Communications Earth & Environment, v. 6, 27, https://doi.org/10.1038/s43247-025-01998-8, 2025.

Giaccio, B., Hajdas, I., Isaia, R., Deino, A., and Nomade, S.: High-precision 14C and 40Ar/39Ar dating of the Campanian Ignimbrite (Y-5) reconciles the timescales of climatic-cultural processes at 40 ka: Scientific Reports, v. 7, no. 1, https://doi.org/10.1038/srep45940, 2017.

Gutenberg, B. and Richter, C. F.: Frequency of earthquakes in California, *Bull. Seismol. Soc. Am.*, 34, 185–188, 1944.

Illsley-Kemp, F., Barker, S. J., Wilson, C., Chamberlain, C. J., Hreinsdóttir, S., Ellis, S., et al.: Volcanic unrest at Taupō Volcano in 2019, *Geochem. Geophys. Geosyst.*, 22, e2021GC009803, https://doi.org/10.1029/2021GC009803, 2021.

Kagan, Y. Y.: Statistics of characteristic earthquakes, *Bull. Seismol. Soc. Am.*, 83, 7–24, https://doi.org/10.1785/BSSA0830010007, 1993.

Lamb, O. D., Bannister, S., Ristau, J., Miller, C., Sherburn, S., Jacobs, K., et al.: Seismic characteristics of the 2022–2023 unrest episode at Taupō volcano, *Seismica*, 3, 1125, https://doi.org/10.26443/seismica.v3i2.1125, 2024.

Lilliefors, H. W.: On the Kolmogorov–Smirnov test for normality with mean and variance unknown, *J. Am. Stat. Assoc.*, 62, 399–402, 1967.

Lilliefors, H. W.: On the Kolmogorov–Smirnov test for the exponential distribution with mean unknown, *J. Am. Stat. Assoc.*, 64, 387–389, 1969.

Malamud, B. D., Turcotte, D. L., Guzzetti, F., and Reichenbach, P.: Landslides, earthquakes, and erosion, *Earth Planet. Sci. Lett.*, 229, 45–59, https://doi.org/10.1016/j.epsl.2004.10.018, 2004.

Marzocchi, W., Spassiani, I., Stallone, A., and Taroni, M.: How to be fooled searching for significant variations of the b-value, *Geophys. J. Int.*, 220, 1845–1856, https://doi.org/10.1093/gji/ggz541, 2020.

Massey, F. J.: The Kolmogorov–Smirnov test for goodness of fit, *J. Am. Stat. Assoc.*, 46, 68–78, https://doi.org/10.1080/01621459.1951.10500769, 1951.

Mele, D., Costa, A., Dellino, P., Sulpizio, R., Dioguardi, F., Isaia, R., and Macedonio, G. Total grain size distribution of components of fallout deposits and implications for magma fragmentation mechanisms: examples from Campi Flegrei caldera (Italy). Bulletin of Volcanology, 82(4), 31., https://doi.org/10.1007/s00445-020-1368-8, 2020.

Natale, J., Ferranti, L., Isaia, R., Marino, C., Sacchi, M., Spiess, V., Steinmann, L., and Vitale, S.: Integrated on-land-offshore stratigraphy of the Campi Flegrei caldera: New insights into the volcano-tectonic evolution in the last 15 kyr: Basin Research, v. 34, no. 2, p. 855–882, https://doi.org /10.1111/bre.12643, 2022.

https://doi.org/10.5194/egusphere-2026-1415
Preprint. Discussion started: 8 April 2026

Natale, J., Vitale, S., Repola, L., Monti, L., and Isaia, R.: Geomorphic analysis of digital elevation model generated from vintage aerial photographs: A glance at the pre-urbanization morphology of the active Campi Flegrei caldera: Geomorphology, v. 460, https://doi.org/10.1016 /j .geomorph.2024.109267, 2024.

Natale, J. and Vitale, S.: Magma chamber failure and dyke injection threshold for magma-driven unrest at Campi Flegrei caldera, *Nat. Commun.*, 16, 7658, https://doi.org/10.1038/s41467-025-62636-7, 2025.

Natale, J., Cascella, E., and Vitale, S.: Tracking the growth and deformation of fissure phreatomagmatic eruptions, *Geol. Soc. Am. Bull.*, 138, 445–468, https://doi.org/10.1130/B38367.1, 2026.

Natale, J., and Vitale, S. Magma chamber failure and dyke injection threshold for magma-driven unrest at Campi Flegrei caldera. Nature Communications, 16(1), 7658, https://doi.org/10.1038/s41467-025-62636-7, 2025.

Newhall, C. G. and Self, S.: The volcanic explosivity index (VEI), *J. Geophys. Res.*, 87, 1231–1238, https://doi.org/10.1029/JC087iC02p01231, 1982.

Orsi, G., D'Antonio, M., de Vita, S., and Gallo, G.: The Neapolitan Yellow Tuff, *J. Volcanol. Geotherm. Res.*, 53, 275–287, https://doi.org/10.1016/0377-0273(92)90086-S, 1992.

Orsi, G., de Vita, S., and Di Vito, M. A.: The restless, resurgent Campi Flegrei nested caldera, *J. Volcanol. Geotherm. Res.*, 74, 179–214, https://doi.org/10.1016/S0377-0273(96)00063-7, 1996.

Orsi, G., Di Vito, M. A., Selva, J., and Marzocchi, W.: Long-term forecast of eruption style and size at Campi Flegrei caldera (Italy), *Earth Planet. Sci. Lett.*, 287, 265–276, https://doi.org/10.1016/j.epsl.2009.08.013, 2009.

Papale, P., Marzocchi, W., and Garg, D.: Global volume distribution for subaerial volcanism on Earth, *J. Geophys. Res. Solid Earth*, 126, e2021JB021763, https://doi.org/10.1029/2021JB021763, 2021.

Pistolesi, M., Bertagnini, A., Di Roberto, A., Isaia, R., Vona, A., Cioni, R., and Giordano, G.: The Baia–Fondi di Baia eruption at Campi Flegrei: stratigraphy and dynamics of a multi-stage caldera reactivation event. Bulletin of Volcanology, 79(9), 67, https://doi.org/10.1007/s00445-017-1149-1, 2017.

Potter, S., Scott, B. J., Jolly, G., Johnston, D., and Neall, V.: A catalogue of caldera unrest at Taupo Volcanic Centre, *Bull. Volcanol.*, 77, 95, https://doi.org/10.1007/s00445-015-0956-5, 2015.

Pyle, D. M.: Sizes of volcanic eruptions, in *The Encyclopedia of Volcanoes*, 2nd ed., edited by H. Sigurdsson, 257–264, Academic Press, https://doi.org/10.1016/B978-0-12-385938-9.00013-4, 2015.

Sandri, L., Costa, A., Selva, J., Tonini, R., Macedonio, G., Folch, A., and Sulpizio, R.: Beyond eruptive scenarios, *Sci. Rep.*, 6, 24271, https://doi.org/10.1038/srep24271, 2016.

Scarpati, C., Cole, P., and Perrotta, A.: The Neapolitan Yellow Tuff, *Bull. Volcanol.*, 55, 343–356, https://doi.org/10.1007/BF00301145, 1993.

Selva, J., Orsi, G., Di Vito, M. A., Marzocchi, W., and Sandri, L.: Probability hazard map for future vent opening at the Campi Flegrei caldera, Italy. Bulletin of volcanology, 74(2), 497-510, https://doi.org/10.1007/s00445-011-0528-2, 2012.

Selva, J., Costa, A., De Natale, G., Di Vito, M. A., Isaia, R., and Macedonio, G.: Sensitivity test and ensemble hazard assessment for tephra fallout, *J. Volcanol. Geotherm. Res.*, 351, 1–28, https://doi.org/10.1016/j.jvolgeores.2017.11.024, 2018.

https://doi.org/10.5194/egusphere-2026-1415
Preprint. Discussion started: 8 April 2026

Simkin, T. and Siebert, L.: *Volcanoes of the World*, Geoscience Press, Smithsonian Institution, 1994.

Smith, V., Isaia, R., and Pearce, N. J. G.: Tephrostratigraphy and glass compositions of post-15 kyr Campi Flegrei eruptions, *Quat. Sci. Rev.*, 30, 3638–3660, https://doi.org/10.1016/j.quascirev.2011.07.012, 2011.

Sparice, D., Pelullo, C., de Vita, S., Arienzo, I., Petrosino, P., Mormone, A., Di Vincenzo, G., Marfè, B., Cariddi, B., De Lucia, M., Vertechi, E., D'Oriano, C., Del Carlo, P., Di Roberto, A., Giaccio, B., Zanchetta, G., and Di Vito, M.A.: The pre-Campi Flegrei caldera (>40 ka) explosive volcanic record in the Neapolitan volcanic area: New insights from a scientific drilling north of Naples, southern Italy: Journal of Volcanology and Geothermal Research, v. 455, https://doi.org /10.1016/j.jvolgeores .2024 .108209, 2024

Sulpizio, R., Costa, A., Massaro, S., Selva, J., and Billotta, E.: Assessing volumes of tephra fallout deposits, *Bull. Volcanol.*, 86, 62, https://doi.org/10.1007/s00445-024-01753-5, 2024.

Wilson, C.: Stratigraphy, chronology, styles and dynamics of late Quaternary eruptions from Taupo volcano, *Philos. Trans. R. Soc. A*, 343, 205–306, https://doi.org/10.1098/rsta.1993.0050, 1993.

Wilson, C.: The 26.5 ka Oruanui eruption, New Zealand, *J. Volcanol. Geotherm. Res.*, 112, 133–174, https://doi.org/10.1016/S0377-0273(01)00239-6, 2001.

Wilson, C., Blake, S., Charlier, B. L. A., and Sutton, A. N.: The 26.5 ka Oruanui eruption, Taupo Volcano, New Zealand: development, characteristics and evacuation of a large rhyolitic magma body, *J. Petrol.*, 47, 35–69, https://doi.org/10.1093/petrology/egi066, 2006.

Wright, H., Pallister, J. S., McCausland, W., Griswold, J. P., Andreastuti, S., et al.: Construction of probabilistic event trees for eruption forecasting at Sinabung volcano, Indonesia 2013–14, *J. Volcanol. Geotherm. Res.*, 382, 233–252, https://doi.org/10.1016/j.jvolgeores.2018.02.003, 2019.